

STUDY ON DISPROPORTIONATION OF TOLUENE ON HZSM - 5 PREPARED FROM RICE - HUSK ASH

A Thesis Submitted
In Partial Fulfilment of the Requirements
for the Degree of

MASTER OF TECHNOLOGY

By
BRIJ BHUSHAN GUPTA

to the

DEPARTMENT OF CHEMICAL ENGINEERING
INDIAN INSTITUTE OF TECHNOLOGY, KANPUR

APRIL, 1988

CERTIFICATE

This is to certify that the present work entitled 'STUDY ON DISPROPORTIONATION OF TOLUENE ON HZSM-5 PREPARED FROM RICE HUSK ASH' has been carried out by Mr. Brij Bhushan Gupta under our supervision and that this work has not been submitted elsewhere for a degree.



Dr. J.K. Gehlawat
Professor



Dr. M. Someswara Rao
Professor

Department of Chemical Engineering
Indian Institute of Technology
Kanpur - 208016

April , 1988

CHE-1988-M-GUP-STV

17 APR 1989
CENTRAL LIBRARY
I. I. T., KANPUR

Acc. No. A104089

7h
660.2915
G4548

ACKNOWLEDGEMENTS

With a great pleasure, I take this opportunity to express a deep sense of gratitude to my thesis supervisors, Prof. M.S. Rao and Prof. J.K. Gehlawat for their inspiring guidance, valuable pieces of advice and meticulous attention in each and every step of this investigation.

I am thankful to my friends and especially Mr. Omar Salim Al-Ayed for his timely help at various stages of this work.

Thanks are also due to Mr. D.N. Mishra, Mr. Samarjee Singh and Mr. D.B. Chakraborty for their timely help.

My sincere thanks go to all those in the department of Chemical Engineering for their kind help.

Brij. B. Gupta

CONTENT

	Page
LIST OF FIGURES	(vi)
LIST OF TABLES	(vii)
NOMENCLATURE	(viii)
ABSTRACT	(ix)
CHAPTER	
1 INTRODUCTION	1
1.1 Introduction	1
1.2 Early choices and new zeolites	2
1.3 Structure and properties of zeolites	3
1.4 Structure and properties of HZSM-5	6
1.5 Shape selective behaviour of HZSM-5	9
1.6 Objectives of the present investigation	10
2 LITERATURE SURVEY	12
3 EXPERIMENTAL	17
3.1 Introduction	17
3.2 Preparation of HZSM-5	17
3.2.1 Chemicals required	17
3.2.2 Procedure	17
3.2.3 Characterization	19

CHAPTER

Page

	3.3	Experimental section	20
	3.3.1	Experimental setup	20
	3.3.2	Input to the reactor	23
	3.3.3	Output from the reactor	24
	3.3.4	Experimental procedure	24
	3.4	Product Analysis	24
4		RESULTS AND DISCUSSION	28
	4.1	Introduction	28
	4.2	Reproducibility of experimental data	29
	4.3	Check for mass transfer effects	30
	4.4	Kinetics and modelling of the main reaction	31
	4.4.1	A pseudo-homogeneous model	31
	4.4.2	A Hetrogeneous model	36
	4.5	p-xylene selectivity	41
5		CONCLUSIONS AND RECOMMENDATIONS	44
		REFERENCES	46
		APPENDICES	48

LIST OF FIGURES

Figure		Page
1.1	The characteristic configuration (a) and its linkage within chains (b) in ZSM-5, (c) channel structure in ZSM-5 zeolite.	7
3.1	X-ray diffraction pattern of ZSM-5 and HZSM-5	21
3.2	Schematic Diagram of the Experiment	22
3.3	Typical Chromatograms	26
4.1	Significance of external diffusional resistance	32
4.2	Effect of particle size on conversion	33
4.3	Toluene conversion vs W/F at various reactor temperatures	34
4.4	Test for reversible second order model	37
4.5	Arrhenius plots for the rate constant	40

LIST OF TABLES

Table		Page
1.1	Physical properties of zeolite ZSM-5	8
3.1	Chemical composition of Rice-husk ash	18
4.1	Reproducibility of experimental data	30
4.2	Homogeneous rate constants	36
4.3	Isothermal regression for the proposed mechanism	41
4.4	Data for p-xylene selectivity at different values of time-on-stream	43

NOMENCLATURE

F	Feed rate of toluene stream, (mol/h)
K_T, K_B, K_X	Adsorption equilibrium constants for toluene, benzene and xylene respectively in the main reaction (atm^{-1})
k, k_1	Rate constants for the main reaction for homogeneous and heterogeneous models respectively, (gmol/h.atm^2)
K	Thermodynamic equilibrium constant for the main reaction
P_T, P_B, P_X	Partial pressures of toluene, benzene and xylene respectively (atm.)
P_{T_0}	Partial pressure of toluene in the feed stream (atm)
$-r_T$	Rate of reaction, (gmol/gcat.h)
T	Absolute temperature
t	Time, h
W	Weight of catalyst in the reactor, g
X	Conversion of toluene

ABSTRACT

The ZSM-5 zeolite synthesized by Rawtani [6] has been converted to its protonated form and toluene disproportionation has been studied on this catalyst. The reaction was carried in a nitrogen atmosphere in a fixed bed differential flow reactor at atmospheric pressure. Mass transfer effects were found to be negligible. The kinetics of the reaction was investigated over a temperature range of 623 K to 773 K. The kinetic data were analyzed on the basis of a second order reversible homogeneous model as well as Langmuir - Hinshelwood mechanism based on adsorption of toluene as the rate controlling step in the overall reaction scheme.

At temperatures lower than 623 K the p-xylene isomer was found to be more than 45% in the xylene mixture. As the temperature was increased to 773 K the p-xylene starts approaching the equilibrium value of 24%. p-xylene was found to be higher than the equilibrium value of 24% through out the study. Thus the synthesized catalyst showed catalytic properties comparable to the commercial HZSM-5 catalyst.

CHAPTER 1

INTRODUCTION

1.1 INTRODUCTION:

Zeolites are gaining utmost importance in recent years due to their use as a molecular sieve as well as a versatile catalyst in a variety of industrially important reactions. They find extensive application in separations and recovery of normal paraffinic hydrocarbons, catalysts of hydrocarbon reactions, drying of refrigerants, separation of air components, curing of plastics and rubber, recovery of radioactive ions from radioactive waste solutions, removal of carbon dioxide and sulfur compounds from natural gas, cryopumping, sampling of air at high altitudes, solubilization of enzymes, separation of hydrogen isotopes, removal of atmospheric pollutants such as sulfur dioxide etc.

Zeolites are also used as molecular sieves and at present, the most important molecular sieve effects are shown by the dehydrated crystalline zeolites. The molecular sieve was proposed by McBain [1] to define porous solid materials which exhibit the property of acting as sieves on a molecular scale. Zeolite molecular sieves have pores of uniform size ($3 \overset{\circ}{\text{A}}$ to $10 \overset{\circ}{\text{A}}$) which are uniquely determined by the unit structure of the crystal. These

pores will completely exclude molecules which are larger than their diameter. Zeolites have high internal surface area available for adsorption due to the channels or pores which uniformly penetrate the entire volume of the solid.

1.2 EARLY CHOICES AND NEW ZEOLITES:

The early developments in the field of zeolites were greatly limited by two factors: first, a limited choice of zeolites the only narrow pore structure readily available was the Linde A zeolite structure ; second, high concentration of Al. sites in a silica zeolite structure prevents the ready conversion and maintenance of protonic sites.

There was a need for synthetic zeolites with high Si/Al ratio and for structure with intracrystalline aperture larger than the 8 - Oxygen ring structure in zeolite A, cabazite, erionite etc. Mordenite was available with some potential for shape selectivity, by a suitable insertion of bulky ions. Mordenite has a linear channel structure with no intersecting pathways. This presented special problems such as single file diffusion creating a tendency for rapid deactivation due to channel obstruction by relatively a few adsorbed molecular entities, or decomposition products. The discovery of methods for zeolite

synthesis using large organic cations as templates in the place of the traditional all inorganic ionic species opened the way to the synthesis of many new zeolites. One of the new zeolites ZSM-5, which belonged to the pentasil group, gave a real breakthrough in the zeolite field. The reason for its success is its exceptional catalytic performance in numerous reactions of industrial importance.

1.3 STRUCTURE AND PROPERTIES OF ZEOLITES:

Zeolites are porous tectosilicate crystals. Their chemistry is based on the tetrahedron TO_4 , where T may be Si or Al. However, all these species are so diverse that secondary building units, based on structural linking of small tetrahedra are needed to describe their topologies. Secondary building unit (SBU) are the smallest number of such units from which the known zeolite topologies can be built. Building up of the crystals with one SBU connected to another gives rise to a regular inorganic crystal with a regular pore structure of precise dimensions. Thus zeolite pores are able to exhibit sieving action on molecules. The pore openings of zeolites range from $2 \overset{\text{O}}{\text{\AA}}$ to $10 \overset{\text{O}}{\text{\AA}}$ which are comparable to most useful organic molecules.

Different types of channel structures are reported for different zeolites. Some zeolites have bidirectional intersecting channels while some others have dual pore systems by having regular pores of two different diameters. Some times these pore channels contain regular cavities of larger size called 'super-cages'. When put into a chemical reaction system, the pore channels in these zeolites provide path for molecular diffusion and sites for reaction. Most of the reactions occur within the pore structure. The fact that acid - catalyzed shape-selective reactions can be achieved over small and medium pore zeolites demonstrates that the acid activity might have originated in the intracrystalline cavities. In the case of hydrogenated zeolites, the protons associated with negatively charged aluminium framework are the sources of Bronsted acid activity for catalysis.

Shape-selective reactions belong to one of the most important class of catalytic reactions of recent interest involving these zeolites of medium-pore type. Due to the shape of the molecule it can either be selected or rejected by the pore channels. The molecules which are capable of entering into the pores as reactants can get converted, those reactions whose transition state molecule can stay

within the pore can only occur and those product molecules which can move out of the pores are the only products of the reaction. Only those reactions will occur in which the shape of reactant molecules, transition state molecules and product molecules altogether satisfy the compatibility of shape. Weisz and Frilette [2] were the first to coin the term 'Molecular shape-selective' reaction. These investigators observed high activity of zeolites 13X and A towards straight chain molecules. Isomeric mixtures of straight and branched chain paraffins, olefins and primary alcohols were taken and reacted over these catalysts. Straight chain molecules were found to be selectively converted leaving branched isomers unreacted. It is assumed that the catalytic activity resides in the extensively developed interstices. These molecular sieve zeolites exclude branched chain molecules that have larger dimensions than the zeolite pore openings.

The availability of medium-pore synthetic zeolites such as ZSM-5, ZSM-11, ZSM-22, ZSM-23, ZSM-35, ZSM-48 has expanded the realm of 'shape selective catalysis'. Branched chain molecules, single-ring aromatics, naphthenes and non-hydrocarbons with critical molecular diameters less than or equal to 6 Å have successfully responded to shape-selective catalysis.

1.4 STRUCTURE AND PROPERTIES OF HZSM-5:

Zeolites can be defined as porous tectosilicate crystals. The chemistry of tectosilicates is based on the tetrahedron TO_4 where T may be either Si or Al. The T atoms of ZSM-5 crystal are practically all Si, being high silica zeolites. However, tectosilicates in zeolites are so diverse that secondary structural units, based on small groupings of linked tetrahedra, are needed in describing and systematizing their topologies. Meier [3] proposed the secondary building units (SBU) as the smallest number of such units from which the known zeolite topologies could be built. The secondary building units of the ZSM-5 framework comprises of 12T atoms (Fig.1.1a). These units join through edges to form chains as shown in Fig. 1.1b. The chains can be connected to sheets and the linking of the sheets lead to a three dimensional framework structure of ZSM-5 zeolite.

The ZSM-5 zeolite structure can exist over a very wide span of compositions, with silica contents approaching 100%. Its least siliceous form has a higher SiO_2/Al_2O_3 ratio than the naturally occurring as well as earlier synthetic zeolites. Many of its physical properties are predominantly dependent on structure and are, therefore, essentially invariant over the entire compositional range while others change with composition in a linear fashion

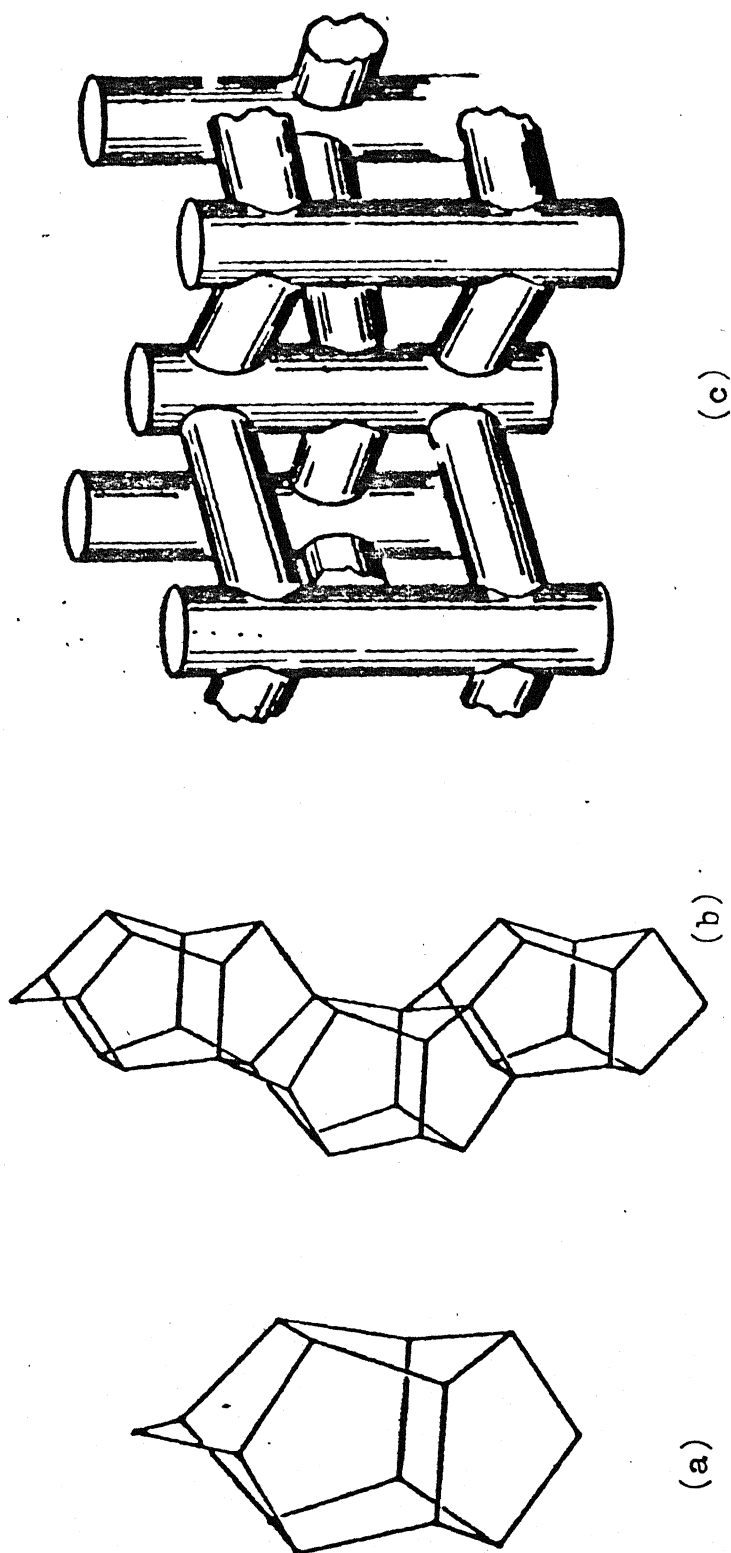


Fig. 1.1: The characteristic configuration (a) and its linkage within chains (b) in ZSM-5. (c) Channel structure in ZSM-5 zeolite (28)

that extrapolates smoothly to the end numbers of the substitutional series, a pure silica ZSM-5. The ZSM-5 series exhibits classical composition related ion-exchange behaviour. However, relative to the traditional zeolites, its ion-exchange capacity is always lower. With the most silicious members, the property may become vanishingly small and ultimately non-existent. In contrast to the classical zeolites, ZSM-5 species are hydrophobic with the degree of hydrophobicity increasing as the aluminium content decreases.

The physical properties of ZSM-5 zeolite are presented in Table 1.1.

Table 1.1: Physical properties of zeolite ZSM-5 [4]

Channel size, Å	
Straight 010	5.4 x 5.6
Sinusoidal 100	5.1 x 5.5
Framework density	
(T atoms/1000 Å ³)	17.9
Refractive Index (25°C)	
As synthesized	1.48
Air calcined at 600°C	1.40
Density (g/cc)	1.77
Micropore volume (cm ³ /g)	0.18
Adsorption volumes	
(at 25°C cm ³ /g)	
n-hexane	0.18
Benzene	0.13

The intersecting channels of a diameter as small as 5 \AA contribute to its catalytic activity, high degree of thermal and acid stability and high selectivity in certain shape-selective reactions. Chen and Garwood [5] reviewed the catalytic properties and applications of HZSM-5. They emphasize on shape selectivity of HZSM-5 which gives rise to some important reactions.

1.5 SHAPE SELECTIVE BEHAVIOUR OF HZSM-5:

In recent years zeolites of the ZSM-family have provided new possibilities affecting the selectivity of catalytic processes. Those molecules which can enter into and come out of the pores are the only reactants and products of a shape-selective reaction. The sharp cut-off point of molecular dimension of about 5 \AA prohibits larger molecules to be either reactants or products. When Na atoms of ZSM-5 are replaced by atoms such as H, Ca atoms or ZSM-5 is impregnated by B,P the crystal changes its coulombic fields and thus the activity and selectivity alter because of the change in sorbing and catalytic properties. Different molecules have different diffusivities because of their configuration. Such diffusion is termed as configurational diffusion, which is observed

in para-selective reactions. However, since ZSM-5 zeolite is most active in its protonated form as the pore ZSM-5 does not have much active sites for acid catalysed reactions, it is either necessary to convert it into hydrogen form or other metallic or non-metallic atoms have to be introduced into it for better catalytic activity.

1.6 OBJECTIVES OF THE PRESENT INVESTIGATION:

As already indicated, ZSM-5 zeolite is most active in its protonated form (HZSM-5) due to the large number of active acid sites as compared to the pure ZSM-5. Recently Rawtani [6] synthesised ZSM-5 in our laboratory using rice-husk ash as the source of silica and alumina, instead of pure chemical sources, used earlier. Rice is the staple food in India and several other countries. Rice-husk, on complete burning yields porous, cellular and light-grey coloured ash (20% dry wt. basis of rice husk) which on analysis has been found to contain amorphous silica up to around 90% by weight of the ash. Being cellular, this silica is in a highly reactive state. As such rice-husk ash is an important source of silica, which on leaching with an alkali like sodium hydroxide offers great potentialities for its use in the synthesis of zeolite catalysts [7,8,9].

Keeping this in mind Rawtani [6] has synthesised ZSM-5 from Na-TPA Cation system using silica and alumina from rice husk-ash. The molar ratio of Si/Al in the husk was 24.88 which was kept constant throughout.

In the present investigation the synthesised ZSM-5 has been converted to a more active form, viz. HZSM-5 and is used to investigate its catalytic properties with a model reaction of toluene disproportionation. This reaction on conventional catalysts gives rise to a low p-xylene content, higher substituted products like trimethylbenzene, tetramethylbenzene and coke. In an uncontrolled reaction a substantial amount of toluene breaks into methane and benzene. The present work has been undertaken to study the catalytic behaviour of HZSM-5 for the model reaction of toluene disproportionation.

CHAPTER 2

LITERATURE SURVEY

The principal raw material presently used for the production of p-xylene, which is used in the manufacture of fiber grade terephthalic acid or the methyl ester, is the C-8 aromatic fraction in the reformat. This consists of a near equilibrium mixture of the three xylene isomers and ethylbenzene. The close boiling points of these compounds and the present high cost of energy have created a situation where only the ortho isomer is separated by distillation. Present commercial methods are based on low temperature crystallization of p-xylene from their mixture [10] or selective adsorption of the para isomer by a molecular sieve. The remaining raffinate is then passed over a catalyst to reequilibrate the xylenes (to 24% para content) for recycling [10]. In addition, it is necessary to transform the ethylbenzene to xylenes and other aromatic compounds with significantly lower or higher boiling points to permit separation by practical distillation methods. This presents the buildup of ethylbenzene in the recycle loop and may lead to a partial conversion to the desired product and other valuable aromatic compounds.

The crude C-8 aromatic fraction from the reformat also contains certain concentration of aliphatic compounds

which have very similar boiling points. A liquid extraction step is used to separate the aliphatic compounds from the aromatic ones, in a primary purification step, so as to prevent eventual buildup of the former in the recycle loop during the p-xylene purification/isomerisation step.

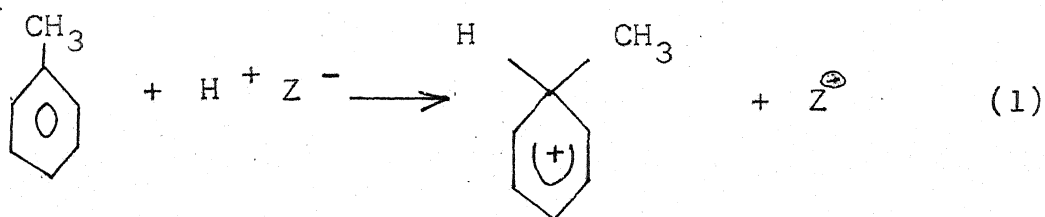
Toluene is also used as a starting material for p-xylene. Processes for disproportionation to benzene and an equilibrium mixture of xylenes over certain solid acid catalysts are available [10].

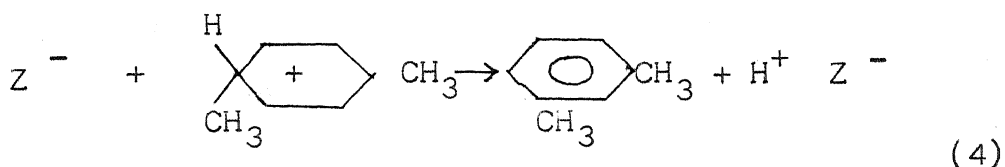
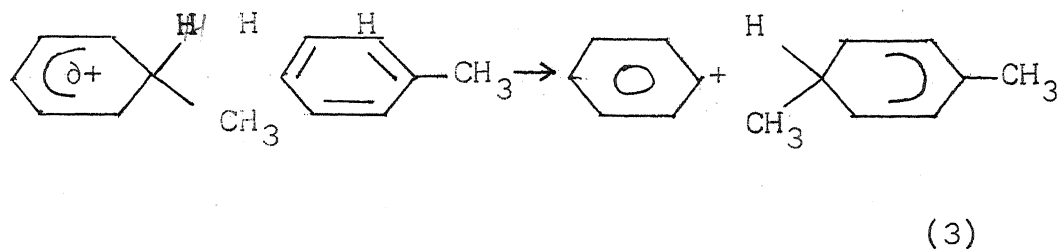
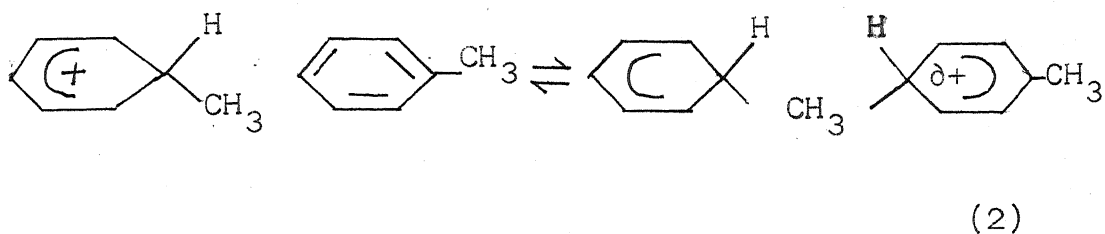
In summary, a number of new process features and options are presently available for the production of fiber grade p-xylene from various starting materials, which reduce energy and production costs and provide flexibility for the use of a variety of aromatic feed stocks available from reformat. Because of configural diffusion, ZSM-5 is more selective to p-xylene and due to the size exclusion higher methanated products and higher aromatics are not produced. This was first studied by Chen et.al.[11]. Kaeding and coworkers [12] increased the acidity of ZSM-5 by converting it into HZSM-5. Subsequently ZSM-5 was modified with phosphorus, boron and magnesium compounds by impregnation techniques. In the reaction products, the xylene fraction

was found to be rich in p-xylene which was as high as 70 - 97% [11,13]. Oxides of these elements reduce the pore openings and channels sufficiently, which leads to an increase of the mean diffusion paths and thus a more pronounced selectivity towards the para product, the isomer with the smallest critical pore dimension.

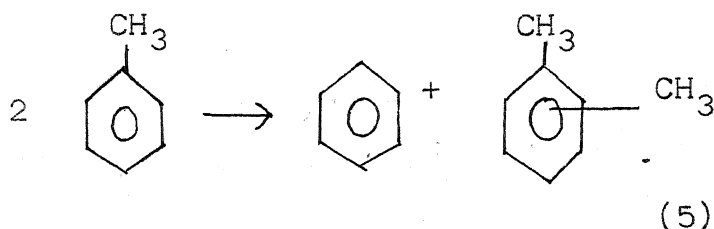
Mechanism of the reaction:

Protonic active sites are the active sites of toluene disproportionation. These active sites can be assumed to be in acidic form of zeolite of bronsted type, $H^+ zeol^-$. It attacks a toluene molecule as shown in Eqn.(1). This weakens the carbon methyl bond and initiates transfer of electrons from a second toluene molecule as shown in Eqn.(3) and a transition state is obtained. This transition molecule because of its configuration can stay in zeolites pores and subsequently breaks as shown in Eqn.(3) to give a benzene molecule and a protonated xylene. Transfer of a proton back to an anionic site of zeolite gives the xylene product and regenerates the active site as shown in Eqn.(4)





Overall reaction:

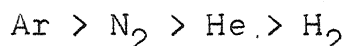


Wei [14] studied the disproportionation reaction using ZSM-5 zeolite as a catalyst, where the diffusivity of para-xylene was thousand times higher than the diffusivities of ortho and meta xylene. The xylene mixture produced in such catalysts from toluene disproportionation can have para-xylene concentrations far in excess of the equilibrium concentrations. He developed a mathematical theory to explain this enhancement of para selectivity and the decline of selectivity under increasing conversion.

Kaeding [15] discussed para selectivity and non-selectivity of xylenes from disproportionation of toluene over HZSM-5 zeolite. Possible mechanisms leading to para selectivity were discussed.

Kürschner and coworkers [16] investigated the effect of thermal treatment of ZSM-5 crystals on its activity. They used this catalyst for toluene disproportionation as well as xylene isomerisation.

Schulz - Ekloff and Jaegar [17] studied the effect of various carrier gases in toluene disproportionation over HZSM-5 at temperature ranging from 300 - 325°C. The conversion was found to be dependent on the type of carrier gas in the order



To sum up, Bronsted acid sites are needed for toluene disproportionation. Increase in the acidity of ZSM-5 increases toluene conversion. Blocking in ZSM-5 pores increases p-xylene selectivity.

In the present study HZSM-5 was used as a catalyst for the disproportionation of toluene.

CHAPTER 3

EXPERIMENTAL

3.1 INTRODUCTION:

In the present study ZSM-5 catalyst prepared by Rawtani [6] has been used to convert it to the hydrogen form of ZSM-5 and further it is used for the disproportionation of toluene. The kinetic data were analysed with a view to test the activity and para-selectivity of HZSM-5 catalyst prepared by using silica and alumina from rice-husk ash. The procedure adopted by Rawtani for the preparation of ZSM-5 is described below.

3.2 PREPARATION OF HZSM-5:

3.2.1 Chemical required: Rice husk ash, tetrapropyl ammonium hydroxide and sodium hydroxide were used as the starting materials for the synthesis of ZSM-5.

3.2.2 Procedure: Initially ZSM-5 was synthesized which was subsequently converted to HZSM-5. Rice-husk obtained from a rice mill in Kanpur was burnt in a muffle furnace at 980°C for 10 h to get carbon free ash. The ash thus obtained was ground to get a particle size of 60 mesh. The chemical composition of the ash is given in Table 3.1.

Table 3.1: Chemical Composition of Rice-husk ash

Components	Percentage(%)
SiO ₂	89.3
Al ₂ O ₃	6.1
Impurities	1.2
Loss on ignition	3.4
Total	100.0

Predetermined amount of sodium hydroxide was added to demineralized water to prepare a sodium hydroxide solution. In another container the required stoichiometric amount of the tetra-propylammonium hydroxide was added to rice-husk ash yielding a viscous TPA-silicate aluminate solution. The alumina used in the reaction was only from the rice-husk ash and no additional alumina was used. The starting mixture had the following molar ratios.

$$\text{SiO}_2/\text{Al}_2\text{O}_3 = 24.88$$

$$\text{TPAO}_2/\text{Al}_2\text{O}_3 = 4.47$$

$$(\text{Na})_2\text{O}/\text{Al}_2\text{O}_3 = 3.4$$

$$\text{H}_2\text{O}/\text{Al}_2\text{O}_3 = 1296$$

The two solutions were mixed, and the autoclave was sealed as quickly as possible to prevent TPA from absorbi

carbon dioxide gas from the atmospheric air. The reaction vessel was placed in a tightly fitting heating assembly fitted with a magnetic stirrer drive. The mixture was stirred for half an hour at room temperature for the gel to form. The reaction was allowed to proceed for 48 h at 175°C. This has been described to be the optimum operating conditions for getting 95% ZSM-5. Experimental details are given by Rawtani [6]. The solid product was filtered under vacuum, washed with demineralized water, and later dried in an oven at 125°C overnight.

To convert ZSM-5 to the hydrogen form of the former was first heated at 550°C for 15 h to decompose the TPA contained in the product, later it was exchanged three times with 1M solution of NH_4Cl solution at 80°C. This converts ZSM-5 to the ammonium form of ZSM-5. The latter was finally calcined at 550°C for 10 h to obtain the Hydrogen form of ZSM-5.

3.2.3 Characterization: The HZSM-5, thus prepared, has been characterized by X-ray diffraction pattern. X-ray diffractograms were obtained on a Seifert diffractometer using Ni-filtered CuK_α radiation. Scanning was carried out in the range of 5 - 50°(2 θ) with a scanning speed (SS) of 3.0°/min and a chart speed (CS) of 6 cm/min. The time

constant and counts per second were maintained at 3 sec and 1 K respectively. The exact peak position were checked by obtaining the counts from point to point within the peak range. When a sample is transformed to the hydrogen form, changes can be observed in the X-ray diffraction patterns (given in Fig. 3.1). One of the prominent changes was the increase in the relative intensity of the first two peaks (at about 7.85 and 8.80 (2θ)) due to the removal of extra framework organic and inorganic species incorporated into the structural voids during synthesis. Because of the same reason the lines at about 11.85 and 12.5 (2θ) decrease in intensity. The doublet centered at about 14.7 (2θ) merges to form an apparent singlet line and the doublet nature of the line at about 23.1 becomes more apparent, and of that at about 23.9 (2θ) becomes less distinct. Detailed characterization techniques are reported by Rawtani [6].

3.3 EXPERIMENTAL SECTION:

3.3.1 Experimental setup: The schematic diagram of the experimental setup used in the present investigation is shown in Fig. 3.2.

A 316 type stainless steel tubular reactor was used for the kinetic studies. The reactor was 1 cm ID and

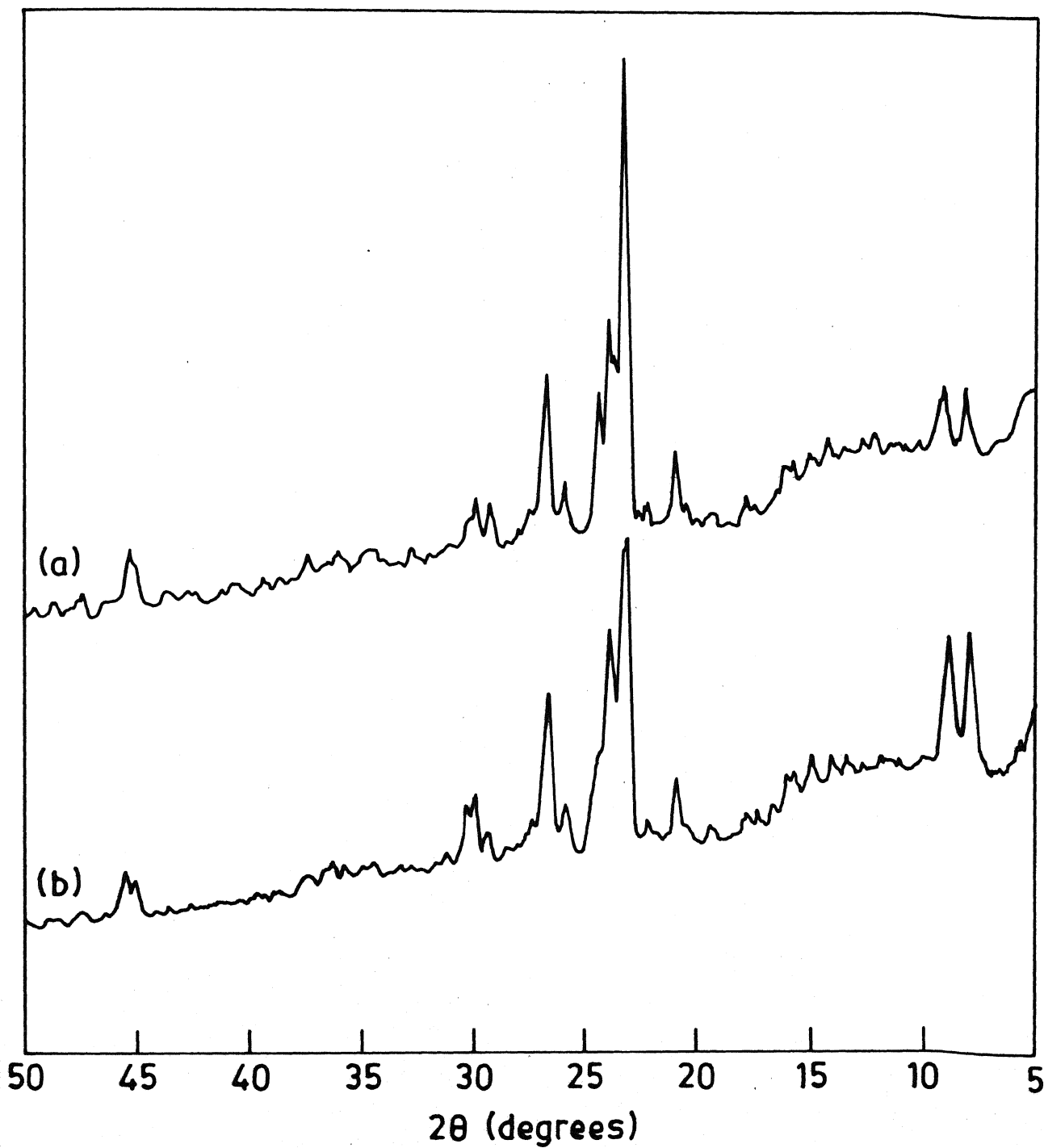


Fig. 3.1. X-ray diffraction pattern of ZSM-5 and HZSM-5.

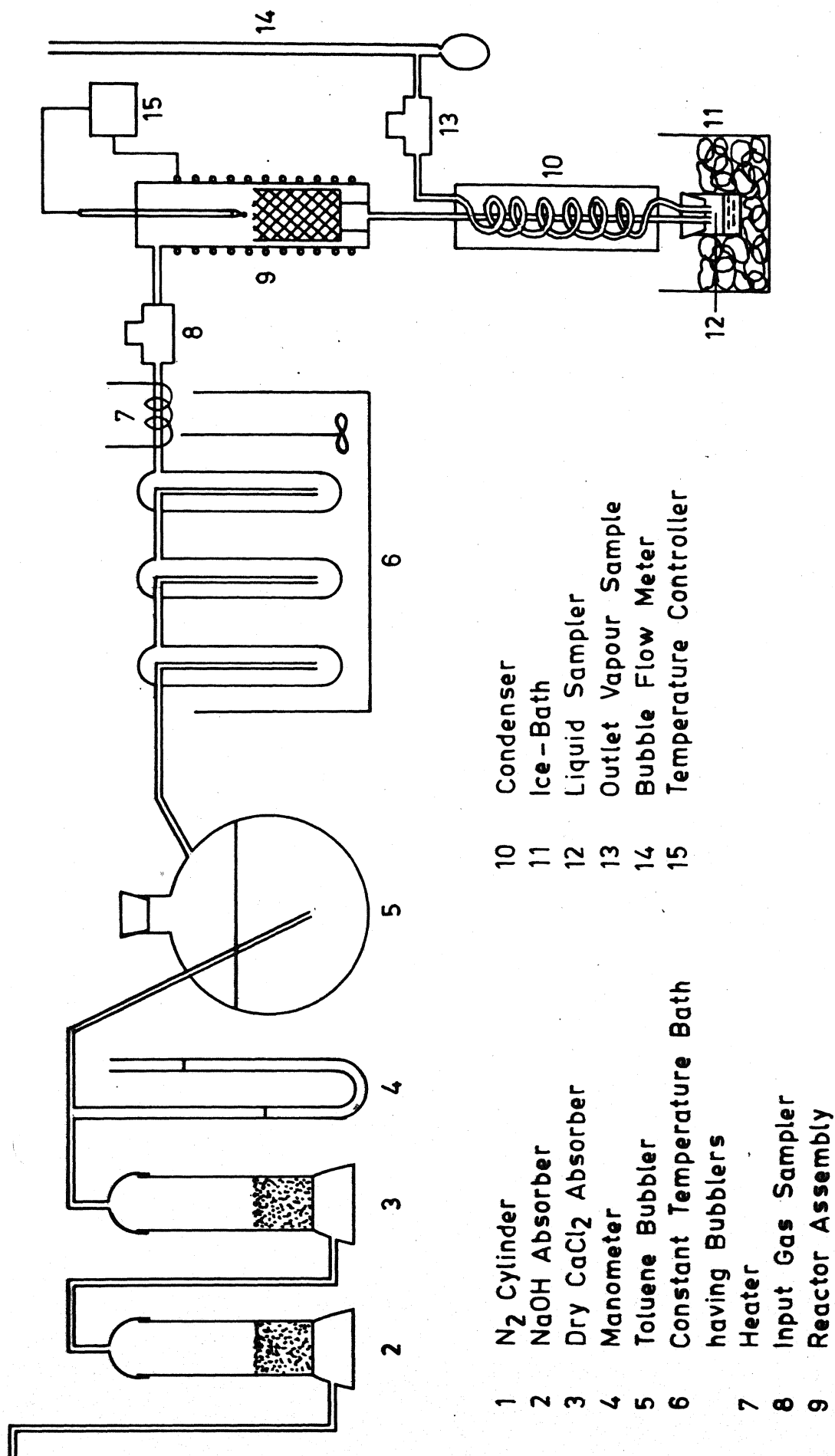


Fig. 3.2. Schematic Diagram of the Experiment.

30 cm long. A thermowell of 22.5 cm depth was installed at the top of the reactor. Chromel-alumel thermocouple was used to measure the temperature of the reactor. The reactor was brought to the desired temperature by an electric heating coil which was insulated by glass-wool and an aluminium foil. The heater was connected to a temperature controller, capable of controlling the temperature to $\pm 2^{\circ}\text{C}$ of the set value.

1.0 g of catalyst was placed inside a tube of 1 cm OD and 6 mm ID over a 120 mesh wire-mesh.

3.3.2 Input to the Reactor: The catalyst was preheated to the desired temperature for 1 h under the flow of nitrogen. Nitrogen gas from a cylinder at a regulated pressure was cleaned by passing it through NaOH pellets and dry calcium chloride. A mercury manometer was installed to provide a visual check to the constancy of the gas flow rate. A soap bubble flow meter was also used to provide a quantitative measure of the flow rate.

The N_2 gas was passed through a series of bubblers kept in a constant temperature bath. A gas sampler was installed at the inlet to get the composition of the inlet gas to the reactor.

3.3.3 The outlet from the Reactor: The vapours from the reactor were passed through an ice-water condenser. Chilled water at a temperature of about 3°C was used as the coolant. The tube was vertically placed in order to drain all the condensate immediately. The liquid product was collected in a sampler kept in a chilled bath. The uncondensed gas was passed through a gas sampler.

3.3.4 Experimental procedure: Nitrogen at a constant flow rate of 50 ml/min saturated with toluene at different temperatures ranging from 50°C to 78°C was fed to the reactor. The experiments in this study were conducted at reaction temperatures ranging between 573 K to 773 K and at a total pressure of 1 atm. The run-time was usually limited to 1 h. No appreciable deactivation of the catalyst was observed during the kinetic runs.

The inlet and outlet gas samples (of 500 μl size) as well as the liquid sample (1 μl size) were analysed by a gas chromatograph.

3.4 PRODUCT ANALYSIS:

A Hewlett Packard (HP 5890A) gas chromatograph fitted with a flame ionization detector was used to analyse the liquid as well as gas products. A 2 mm I.D., 3.2 mm O.D. and 3 m long stainless steel column packed with

5% Bentone - 34 and 5% diisodecyl phthalate on chromo-sorb-W was used for chromatographic analysis. The best operating conditions were obtained after several trial runs. They are listed as below:

Sample volume : 1 μ l of liquid
500 μ l of gas
Column temperature : 110°C
Detector temperature: 140°C
Injector temperature: 200°C
Carrier gas flow rate(N): 25 ml/min
H₂ flow rate : 25 ml/min
High-purity air flow rate: 80 ml/min

A typical chromatogram showing the separation of various peaks is shown in Figure (3.3). The various products were benzene, toluene, O-xylene, p-xylene, m-xylene, trimethylbenzene and methane. A mixture containing known amounts of the above components was analysed under the same column conditions. The peak areas of components were not directly proportional to the percent composition i.e. different compounds had different detector responses. Thus the detector response factors [18] were used to get the percent composition. The various detector response factors are listed below:

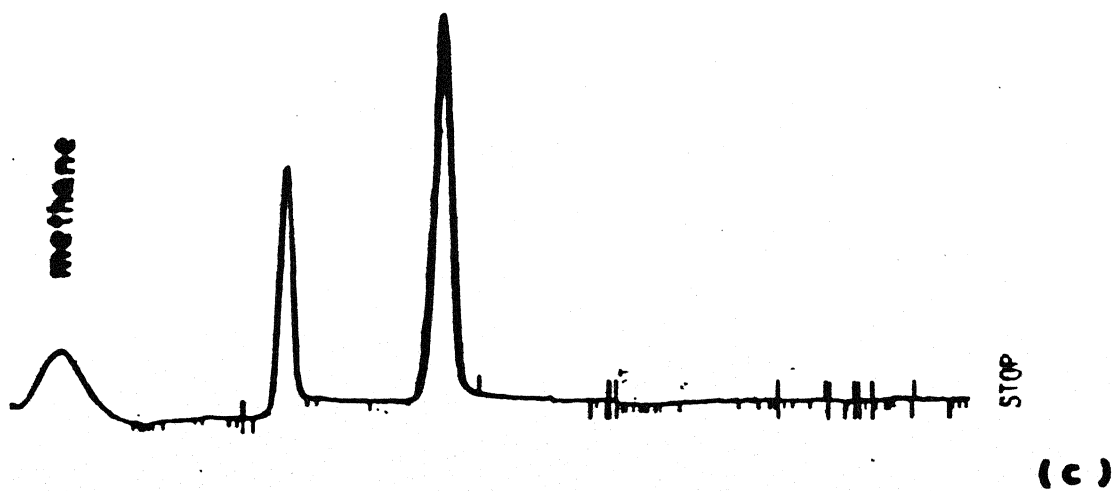
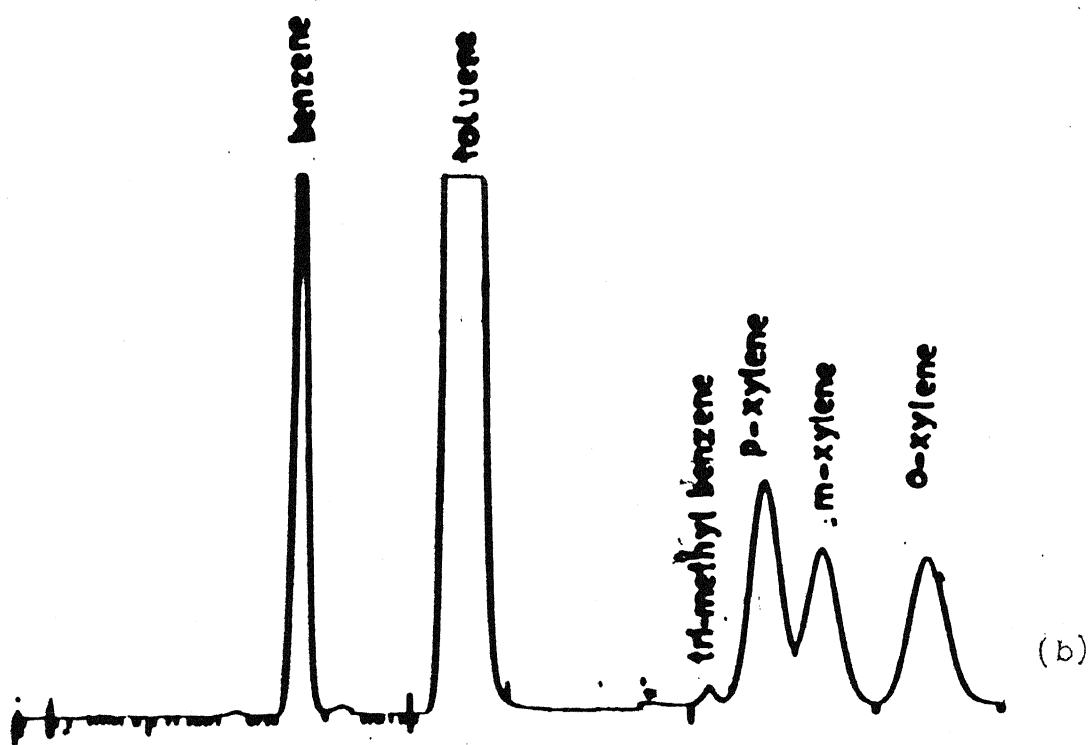
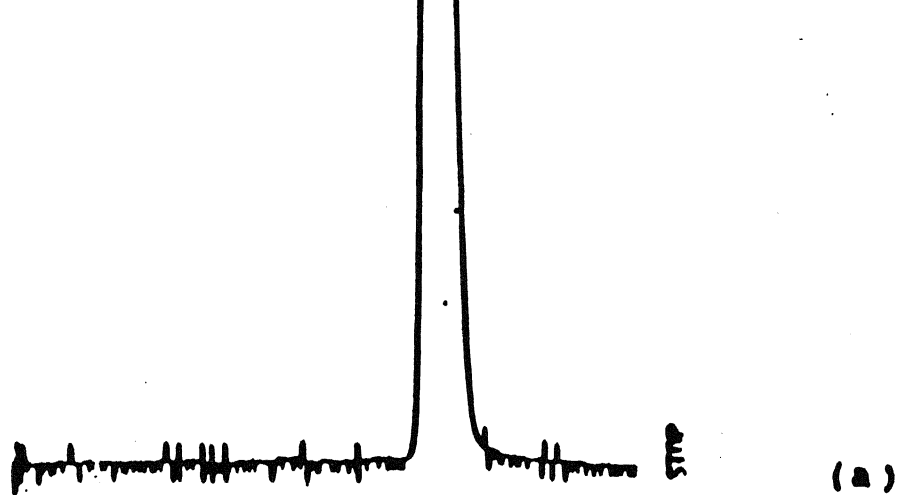


FIG 3.3 Typical Chromatograms (a) Toluene Input Composition

<u>Component</u>	<u>Detector response factor</u>
Methane	0.952
Benzene	1.12
Toluene	1.07
P-xylene	1.00
O-xylene	1.04
m-xylene	1.02
triethylbenzene	1.05

CHAPTER 4

RESULTS AND DISCUSSION

4.1 INTRODUCTION:

The experiments in this study were conducted at reaction temperatures ranging between 573K to 773K and at a total pressure of 1 atm. The run time was usually limited to 2 h. Nitrogen was used as a carrier gas. After every run the catalyst was regenerated under O₂ supply at 573K for 5 h. To study the kinetics of the main reaction, runs were conducted at 4 different temperatures (623K, 708K, 723K, 773K) and the partial pressure of the reacting components were varied by changing the temperature of the bubblers. The catalyst was stable for 1 h giving constant conversion and the kinetic data were taken at conditions, where catalyst deactivation was not predominant.

Studies were made with the thus synthesised HZSM-5 zeolite catalyst to determine potential for disproportionation of toluene. The results with HZSM-5 zeolite, at various temperatures, are shown in Appendix-1. Toluene conversion increased in direct proportion to the temperature from 3.3 to 12.4% in the range of 623K to 773K. At the lowest temperature, the mole ratio of benzene/xylenes was

close to the theoretical value of 1.0. The observed ratio increased with increase in temperature to a value of 1.06 at 773K. This was primarily due to demethylation reaction as indicated by the corresponding increase in the yield of methane. Only a small amount of transalkylation occurred to give C_9^+ aromatics. A near equilibrium mixture of xylene isomers was obtained at 773K.

Wei [23] theoretically predicted that the xylene mixtures produced by alkylation or toluene disproportionation reaction using above modified catalysts can have p-xylene concentration much above the equilibrium value. This p-selectivity will be more at low conversion and lowers down at higher conversion. The slight preference of p-xylene at low conversions may be understood in terms of a transition state selectivity where the product can leave the channel system of zeolite before the equilibrium is reached.

4.2 REPRODUCIBILITY OF EXPERIMENTAL DATA:

The reproducibility of experimental data was checked by repeating the experiments under exactly the same reaction conditions. The data (Table 4.1) were reproducible within an error of $\pm 5\%$.

Table 4.1: Toluene disproportionation over HZSM-5
catalyst prepared from Rice-husk ash.

	Run			
	5	16	25	26
Temperature, K	623	773	623	773
Pressure, atm.	1	1	1	1
Weight of cat. ^a ,g	1.0	1.0	1.0	1.0
Toluene, WHSV ^b	5.2	9.27	5.2	9.27
Conversion, %	2.6	7.0	2.8	6.8

a - 3 mm pellet

b - Weight hourly space velocity: weight of feed per unit weight of catalyst per hour.

4.3 CHECK FOR MASS TRANSFER EFFECTS:

It is important that mass transfer effects should be absent during the reaction in a fixed bed catalytic reactor to ensure the intrinsic kinetics. Both external as well as intra-particle effects, were checked in the present study before the kinetic data were taken. Effect of external diffusion on conversion was studied by conducting two runs with a fixed W/F (g cat.h/mol) ratio but varying

the weight of the catalyst. Since the mass transfer resistances are more likely to effect the reaction at high temperatures, these preliminary runs were performed at the maximum temperature (773K) used for the main runs. The conversion vs W/F data (Appendix-¹~~1~~) for these runs are plotted in Fig.4.1. The experimental data of both the runs follow a single curve and hence it can be concluded that external mass transfer effects are unimportant and can be neglected.

Similarly, to check for pore diffusional limitations, a series of runs were made with different sizes of pellets at otherwise identical conditions. The results (Appendix-¹~~1~~) presented in Fig. 4.2 show that the conversion remained constant for different particle sizes, indicating thereby that the pore diffusional resistances were negligible. Another test was conducted to check for any catalytic effect of the reactor wall but no reaction was observed (data not presented).

4.4 KINETICS AND MODELLING OF THE MAIN REACTION:

4.4.1 A Pseudohomogeneous Model: The conversion vs W/F data for the four different temperatures (623K, 708K, 723K and 773K) are shown in Fig.4.3. The data are presented in Appendix -¹~~1~~. The kinetic data were analyzed using

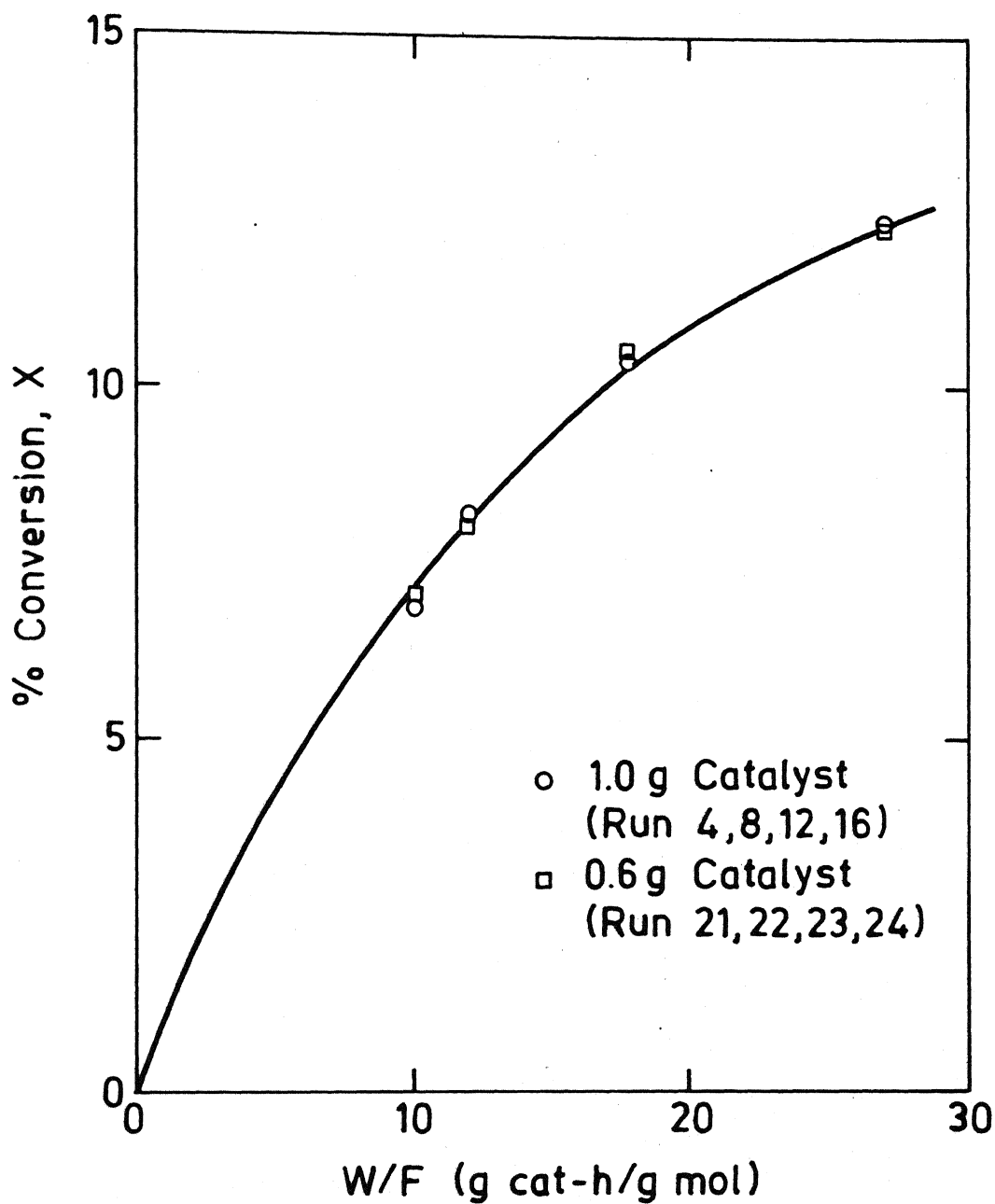


Fig. 4.1. Significance of external diffusional resistance.

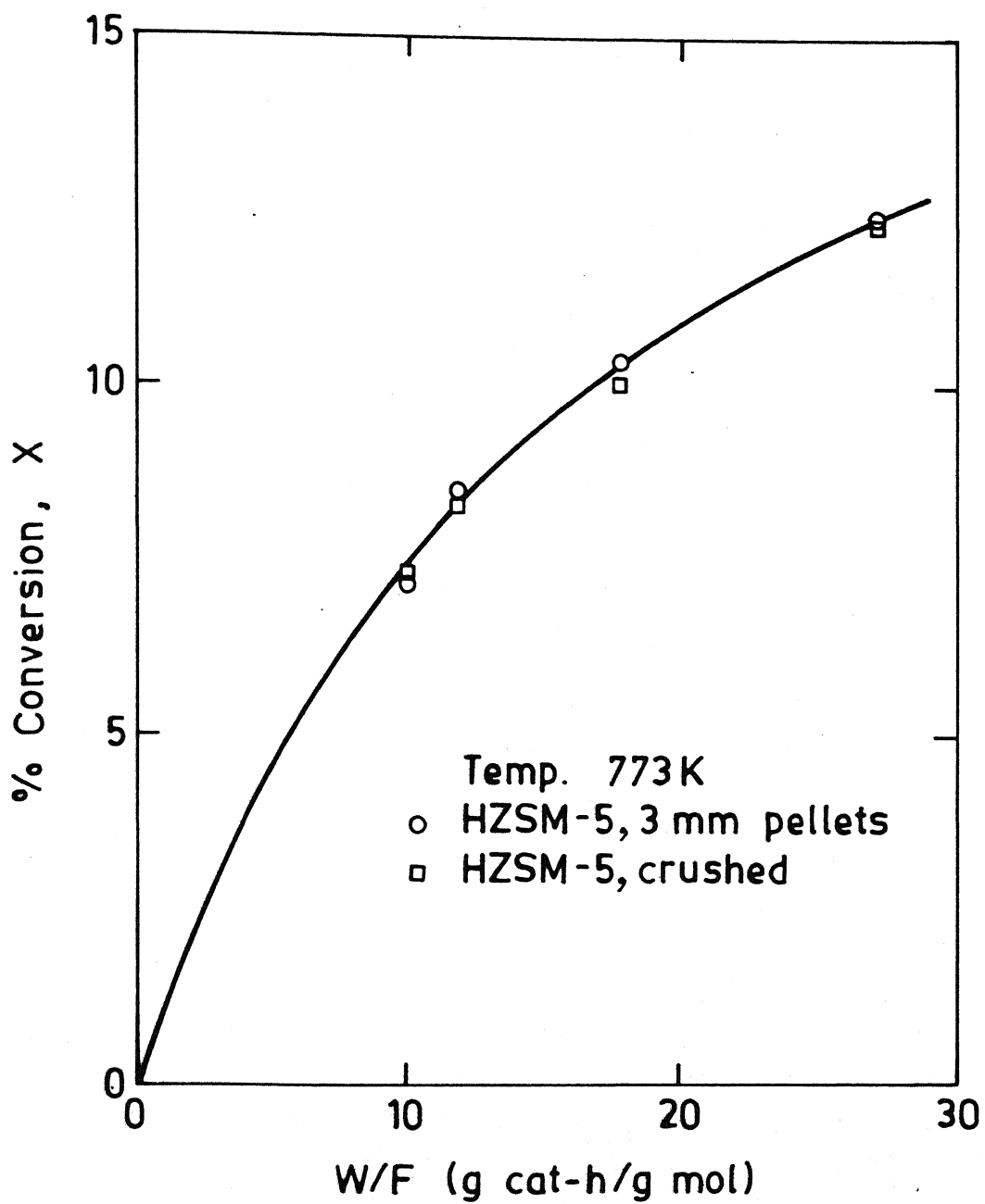


Fig. 4.2. Effect of particle size on conversion.

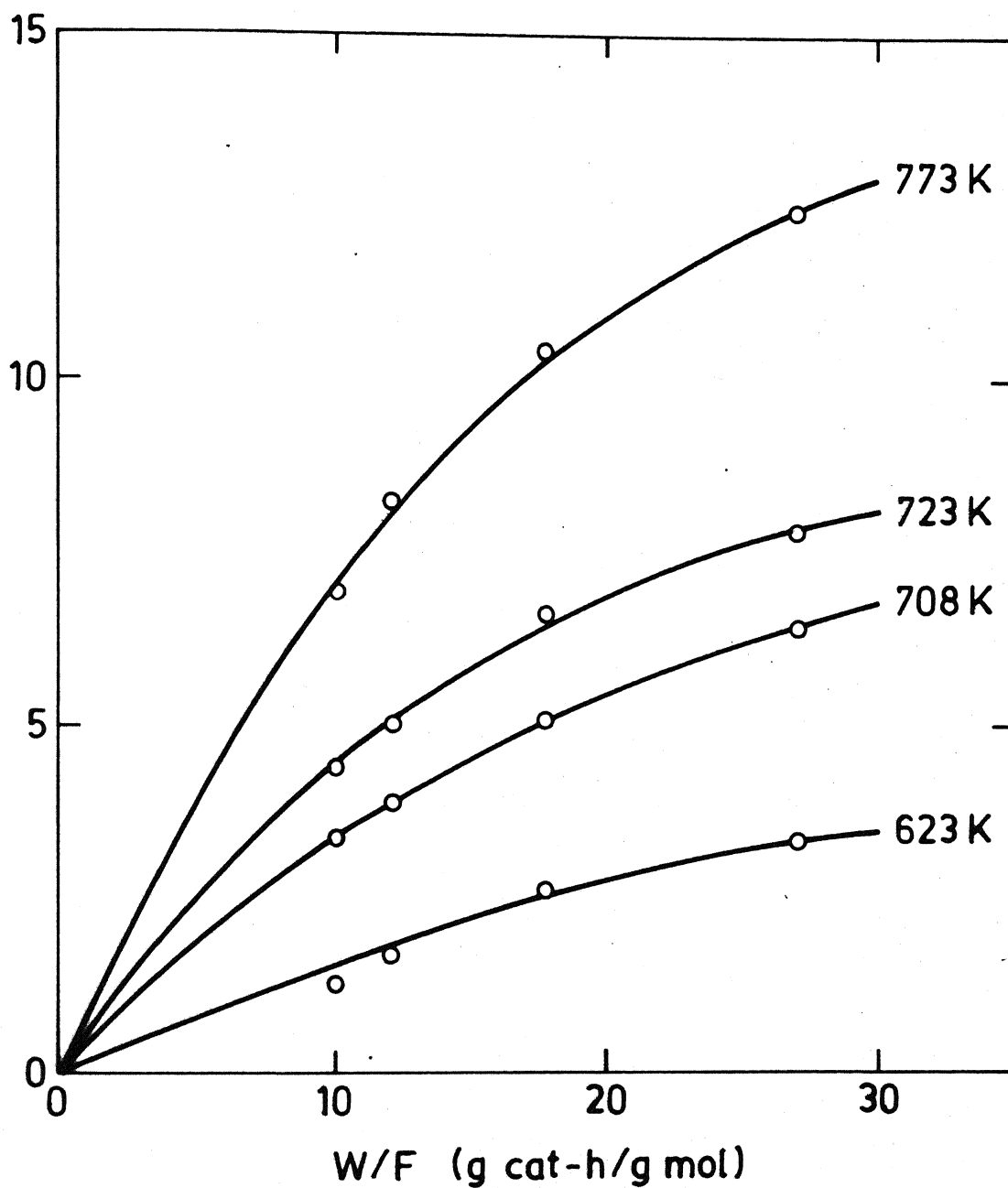
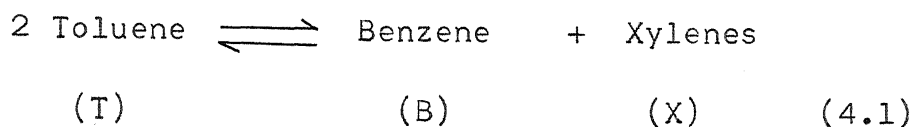


Fig. 4.3. Plots of Toluene conversion vs W/F at various reactor temperatures.

both homogeneous and heterogeneous models as discussed below.

The disproportionation of toluene to benzene and xylene can be represented on the catalyst surface as



A homogeneous model based on second order reversible reaction was also proposed by Sridhar and Patwardhan for toluene disproportionation [19].

The rate of reaction, expressed as gmol of toluene disappeared per hour per gram of catalyst is represented as follows:

$$\text{rate: } \frac{-dF}{dW} = k (P_T^2 - P_B P_X / K) \quad (4.2)$$

Integrating the above expression will give [19]

$$\frac{W}{F} = \frac{K^{1/2}}{k P_{T_0}^2} \left[\ln \left| \frac{2AX + B - (1/K)^{1/2}}{2AX + B + (1/K)^{1/2}} \right| - \ln \left| \frac{B - (1/K)^{1/2}}{B + (1/K)^{1/2}} \right| \right] \quad (4.3)$$

where $A = 1 - 1/4K$, $B = -2.0$

The kinetic data were analyzed using Eq.(4.3) where the equilibrium constant for toluene disproportionation was calculated by using the free energy data²⁰[20] and were found to be in a close range of 12.85 to 13.16 for a temperature range of 708K to 773K. Fig. 4.4 shows the validity of the Eq.(4.3). These data show a linear relationship confirming the validity of the reversible second order rate model. The rate constant at different temperatures are calculated from the slopes of the linear plots in Fig. 4.4 and are given in Table

Table 4.2: Homogeneous rate constants.

Temp. K	k, gmol/h(atm.) ²
708	0.08
723	0.1636
773	0.3636
623	0.945

4.4.2 A Hetrogeneous Model: A hetrogeneous model was proposed for the present reaction based on Langmuir-Hinshelwood mechanism. The reaction steps, involved in this mechanism, are assumed to be as follows:

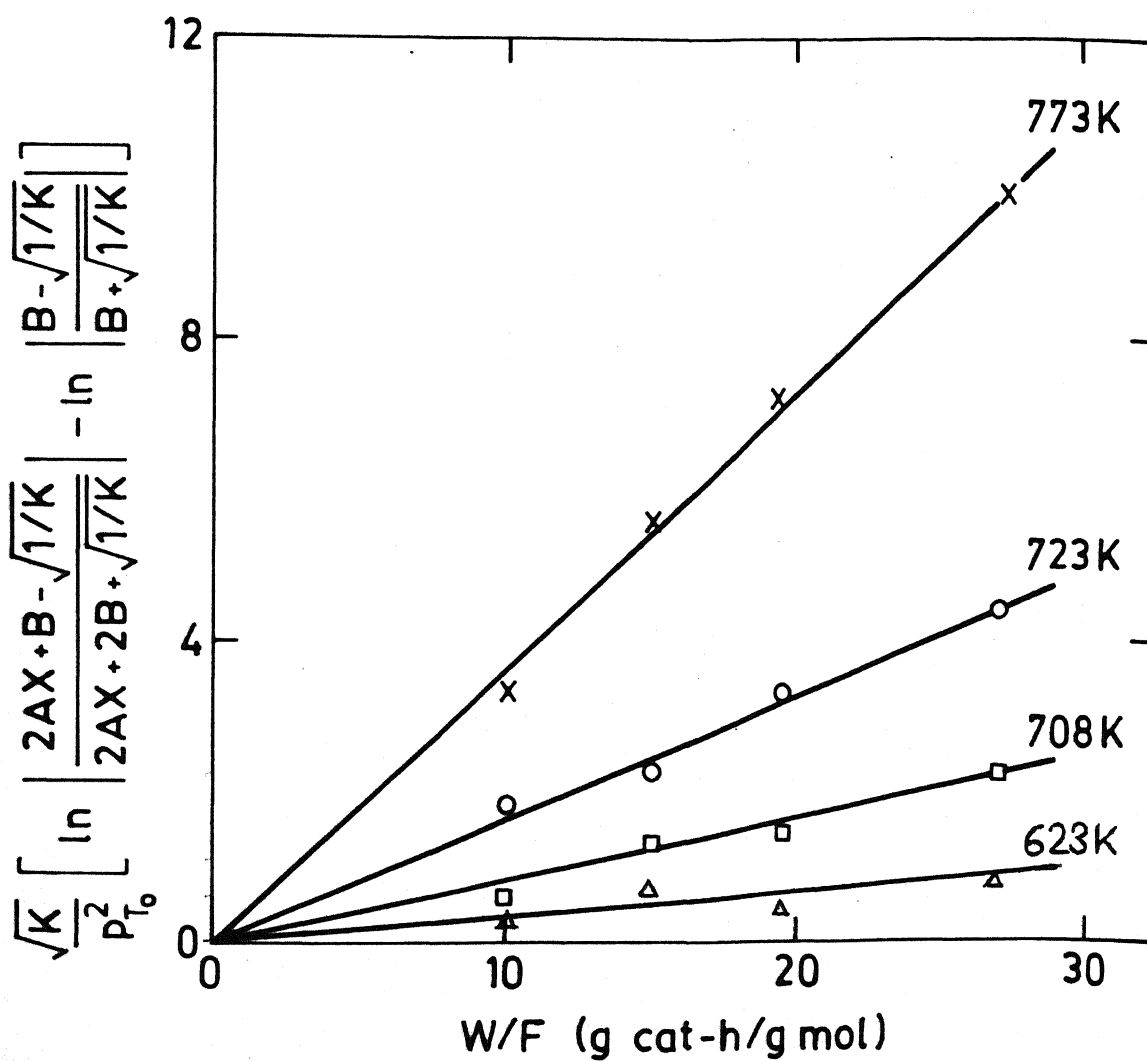


Fig. 4.4. Test for reversible second order model.

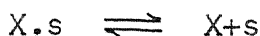
1. Toluene is adsorbed on the surface of catalyst



2. Surface reaction between adsorbed reactants.



3. Desorption of the products from the surface.



The derived rate expression based on adsorption of toluene as rate controlling, for the proposed model is given by (Appendix-2). 1.5

$$-r_T = \frac{k_1(P_T - \sqrt{P_B P_X / K})}{(1 + K_T \sqrt{P_B P_X / K} + K_B P_B + K_X P_X)} \quad (4.7) \quad u.7$$

where P_T, P_B, P_X are the partial pressure of toluene, benzene and xylene respectively, (Appendix-3)

K_B, K_T, K_X are the adsorption equilibrium constants for benzene, toluene and xylene respectively, and k_1 is the absorption rate constant.

A non-linear regression algorithm (available in the NAG subroutines) utilizing Gauss - Newton and quasi-Newton methods was used to obtain the parameters in the rate expressions. The program is listed in Appendix- 5.

The model discrimination was done based upon the requirement that kinetic and adsorption constants had to be positive.

The kinetic parameters evaluated from heterogeneous model are shown in Table 4.3. The rate constants and adsorption equilibrium constants turned out to be positive for the case of adsorption of toluene as the rate-controlling step. The former turned out to be negative in the case of surface reaction as rate-controlling step. Thus, it is assumed only the former mechanism is plausible. The rate constant k_1 was plotted against reaction temperature in the form of an Arrhenius plot as shown in Fig. 4.5. The rate constants evaluated from the homogeneous model were also plotted in Fig. 4.5 for comparison. The activation energies were determined from the slopes of Fig. 4.5. Dependency of the kinetic parameters on temperature was determined by the following expressions.

$$\begin{aligned}
 k &= 32859 \exp \left(- \frac{9000}{T} \right) \\
 k_1 &= 3 \times 10^{16} \exp \left(\frac{-29000}{T} \right)
 \end{aligned}
 \tag{4.8}$$

The activation energy as determined by the slopes of the Arrhenius plots (Fig. 4.5) is equal to 17.883 kcal/mo.

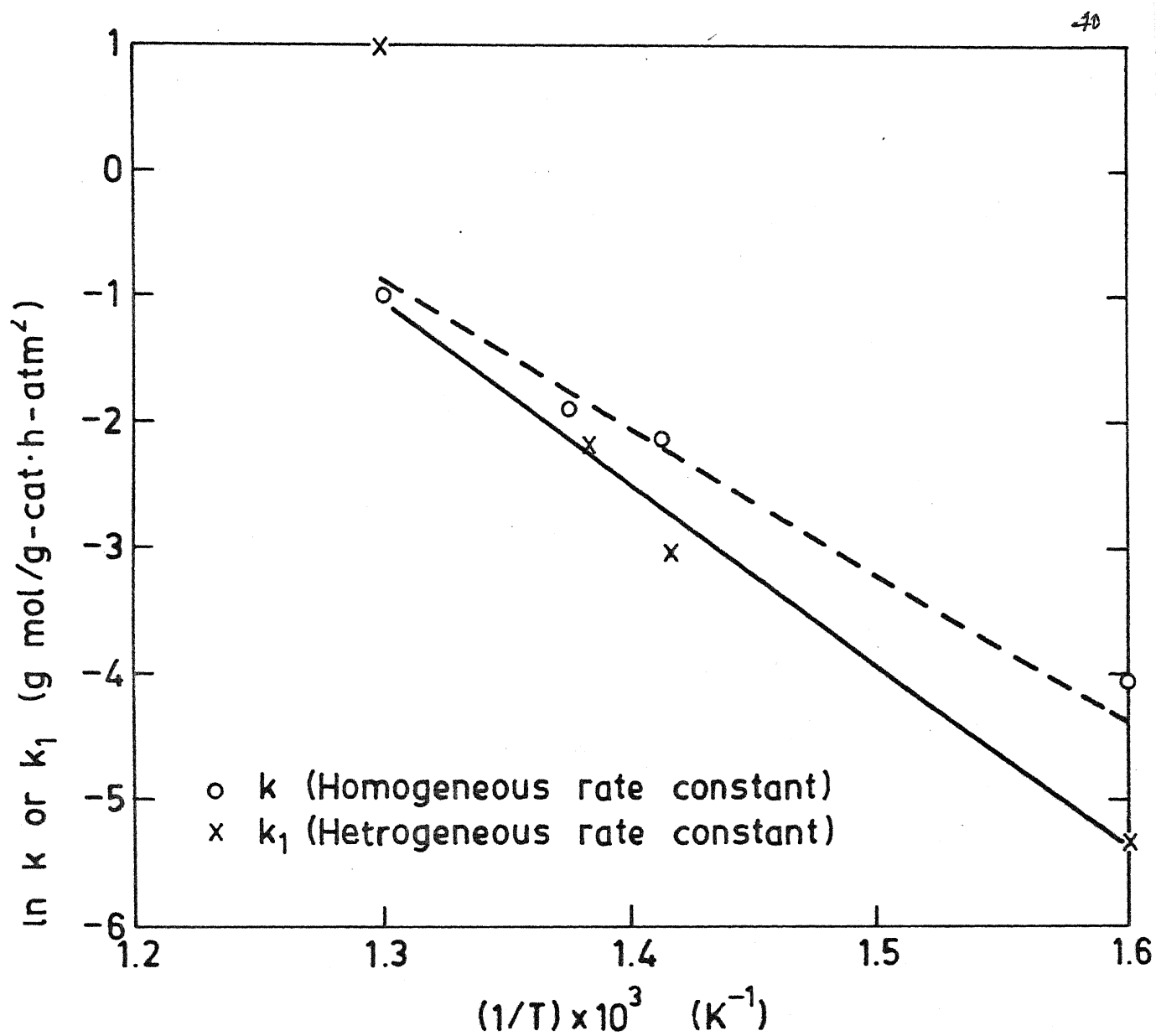


Fig. 4.5. Arrhenius plots for the rate constants.

in case of homogeneous model and 57.62 kcal/mol in case of heterogeneous model. At high temperatures the activation energy seems to be different than that determined at low temperatures, It is possible that there is a shift in the reaction mechanism. An activation energy of 14.5 kcal/mol for silica-alumina catalyst (Izumi and Shiba, 1963) [19] has been reported in literature. Kaeding et.al.[13] reported an activation energy of > 20 kcal/mol for toluene disproportionation.

Table 4.3: Isothermal regression for the proposed mechanism.

Temp. (K)	k_1 (gmol/h atm ²)	K_T (atm ⁻¹)	K_B or K_X (atm ⁻¹)
623	4.89×10^{-3}	17210	1062.8
708	4.73×10^{-2}	6780.5	913.75
723	1.108×10^{-1}	5220.0	813.5
773	3.064	1445.6	610.9

4.5 P-XYLENE SELECTIVITY:

An important aspect of toluene disproportionation reaction is the p-xylene selectivity. To assess the effect of the channel width and channel structure upon p-selectivity an analysis of the ratios of p-xylene and the sum of the

xylenes has been carried out for a few experiments. The results of this analysis are shown in Tab. 4.4. The p-xylene selectivity has been found to be more than its equilibrium value. It is observed [10] that a dramatic increase in the amount of para isomer produced in the xylene product occurred with catalysts that had been modified for eg. HZSM-5 (Table 1). It has been proposed that the para isomer, by virtue of its relatively small minimum dimension, is able to diffuse out of the catalyst at rates greater than three orders of magnitude faster than the meta and ortho isomers [11, 21]. A plausible explanation is that the pores in the ZSM-5 zeolite are approximately 7.8 \AA in diameter, which permit the rapid diffusion of toluene and para-xylene with molecular diameters of 6.3 \AA , but severely retard the diffusion of ortho and meta-xylenes with molecular diameters of 6.9 \AA [12,22] and thus ortho and meta-xylene, because of their longer residence times within the pores, have the opportunity to isomerise to para-xylene before diffusing out of the catalyst pores. This effect has been explained by Kaeding et al.[11,13]and by theoretical considerations by Wei et al.[23,24].

Table 4.4: Data for p-xylene selectivity

Reactor Temp. - 773 K

WHSV - 3.3 h⁻¹

Time (min)	Wt.%				
	Benzene	Toluene	p-X	m-X	o-X
30	6.14	87.6	1.80	3.08	1.38
45	5.61	88.62	1.687	2.84	1.25
60	5.25	89.203	1.64	2.71	1.197
75	5.8	89.5	1.728	2.84	1.24
90	5.72	88.453	1.68	2.94	1.20
105	5.12	89.543	1.61	2.60	1.11

$$\text{p-xylene selectivity} = \frac{\text{amount of p-xylene formed}}{\text{amount of total xylenes formed}}$$

CHAPTER 5

CONCLUSIONS AND RECOMMENDATIONS

CONCLUSIONS:

The following conclusions can be made from this study.

1. The synthesised HZSM-5 zeolite catalyst gave activity and conversions comparable to those reported by earlier investigators[^{12, 23}13,23]
2. The kinetic data of toluene disproportionation were most satisfactorily correlated by the homogeneous model and a heterogeneous model as well, which assumes the adsorption of toluene on the catalyst surface as the rate controlling step.
3. The 'as synthesised HZSM-5' catalyst showed higher p-xylene selectivity. Similar observations were found by Keating et al.[²³13] and Wei [23].

RECOMMENDATIONS:

1. Toluene disproportionation reaction may be studied using modified HZSM-5 after impregnation with boron or phosphorus etc.

2. Deactivation studies may be carried out.
3. The present study was limited to low partial pressures of toluene. The reaction may be studied at higher partial pressures of toluene.

REFERENCES

1. McBain, J.W., 'The sorption of gases and vapours of solids, Chap. 5, Rolledge and sons, London (1932).
2. Weisz, P.B. and Frilette, V.J., Journal of Phys.Chem. 64, 382 (1960).
3. Meier, D.J., 'Molecular basis of transition and relaxations', 1978.
4. Olson, D.H., Haag, W.D., Lago, R.M., J. of catalysis, vol 61, 390 (1980).
5. Chen, N.Y., and Garwood, W.E., Cat.Rev.Sc.Eng. 28(283), 85 (1986).
6. Rawtani, A.V., synthesis and characterization of zeolite ZSM-5 prepared using silica from Rice-husk ash, M.Tech thesis, IIT Kanpur (1986).
7. Bajpai, P.K., Rao, M.S., Gokhale, K.V.G.K., Ind. Eng. Chem. Prod. Res. Dev., vol 17, 223 (1978).
8. Bajpai, P.K., Rao, M.S., Gokhale, K.V.G.K., Ind. Eng. Chem. Prod. Res. Dev., vol 20, 721 (1981).
9. Dalai, A.K., Rao, M.S., Gokhale, K.V.G.K., Ind. Eng. Chem Prod. Res. Dev., 24, 465 (1985).
10. Kaeding, W.W., Chu, C., Young, L.B., Weinstein, B., and Butter, S.A., J. of Appl. Polymer Science, 36, 209-215 (1981).
11. Chen, N.Y., Kaeding, W.W., Dwyer, F.G., J. Amm.Chem.Soc. 101, 6783 (1979).
12. Kaeding, W.W., Chu, C., Young, L.B., Weinstein, B., and Butter, S.A., J. Catal. 67, 159 (1981).
13. Young, L.B., Butter, S.A., and Kaeding, W.W., J. of Cat. 76, 418 (1982).
14. Theodorou, D., Wei, J., J of Catal. 83, 205 (1983).
15. Kaeding, W., J.Catal 76, 418 (1982).
16. Kruschner, U., Parlitz, B., Schreier, E., Ohlmann, G., Volter, J. Appl Catalysis, 30, 159 (1987).

17. Schulz, G., Ekloff and N.J. Jaegar, Applied catalysis, 33, 73 (1987).
18. McNair, H.M., and Bonelli, E.J., Basic Gas Chromatography (1969).
19. Sridhar, S.B., Patwardhan, S.R., Ind. Eng. Chem. Prod. Res. Dev. 20, 102 (1981).
20. Chemical Engineers handbook, Perry, R.H., Chilton, C.H., Vol.5 (1985).
21. Mavrodinova, V., Ch. Minchev and V. Penchev, zeolites, 1985, vol.5, July 217
22. Kaeding, W.W., Chu, C., Young, L.B., and Butter, S.A., J. catal. 69, 392 (1981).
23. Wei, J., J of Catal 1982, 19, 213.
24. Wei, J., J. of Catal 1982, 76, 433

APPENDIX-1Experimental data on toluene disproportionation over
HZSM-5 Catalyst

	Run			
	1	2	3	4
Temperature, K	623	708	723	773
Pressure, atm.	1	1	1	1
Wt. of cat. ^a , g	1.0	1.0	1.0	1.0
Toluene, WHSV ^b	3.3	3.3	3.3	3.3
Conversion	3.3	6.4	7.8	12.4
Product, wt. %				
CH ₄	-	-	-	Traces
Benzene	1.612	3.2	3.27	6.34
Toluene	96.712	93.59	92.2	87.62
Ethylbenzene	-	-	-	Traces
P-xylene	0.730	1.28	1.60	1.64
Meta-xylene	0.672	1.61	2.27	3.02
O-xylene	0.268	0.320	0.639	1.32
Xylene Isomers, %				
Para	43.71	39.8	35.6	27.42
Meta	40.23	50.15	50.25	50.5
Ortho	16.04	9.96	14.15	22.07

a - 3 mm pellet

b - Weight hourly space velocity: weight of feed per unit weight of catalyst per hour.

APPENDIX-1 (Continued)

	Run			
	5	6	7	8
Temperature, K	623	708	723	773
Pressure, atm.	1	1	1	1
Weight of cat. ^a , g	1.0	1.0	1.0	1.0
Toluene, WHSV ^b	5.2	5.2	5.2	5.2
Conversion, %	2.6	5.1	6.6	10.4
Product, wt. %				
CH ₄	-	-	Traces	Traces
Benzene	1.48	2.28	2.94	5.88
Toluene	93.37	94.90	93.40	89.58
Ethylbenzene	-	-	-	Traces
P-xylene	0.517	1.022	1.244	1.26
m-xylene	0.530	1.413	1.755	2.25
o-xylene	0.072	0.384	0.639	1.00
Xylene Isomers, %				
Para	46.20	36.26	34.20	27.92
Meta	47.34	50.12	48.23	49.80
Ortho	6.46	13.62	17.57	22.28

a - 3 mm pellet

b - Weight hourly space velocity: weight of feed per unit weight of catalyst per hour.

APPENDIX-1 (Continued)

	Run			
	9	10	11	12
Temperature, K	623	708	723	773
Pressure, atm.	1	1	1	1
Weight of cat. ^a , g	1.0	1.0	1.0	1.0
Toluene, WHSV ^b	7.78	7.78	7.78	7.78
Conversion, %	1.7	3.9	5.0	8.3
Product, wt. %				
CH ₄	-	-	-	Traces
Benzene	0.83	1.37	2.18	4.313
Toluene	98.3	96.1	95.0	91.7
Ethylbenzene	-	-	-	Traces
p-xylene	0.409	1.02	1.10	1.19
m-xylene	0.416	1.26	1.46	1.96
o-xylene	0.02	0.236	0.432	0.837
Xylene Isomers, %				
Para	47.65	40.54	30.67	29.85
Meta	48.43	50.07	48.56	49.16
Ortho	3.90	9.37	20.77	20.99

a - 3 mm pellet

b - Weight hourly space velocity: weight of feed per unit weight of catalyst per hour.

APPENDIX-1 (Continued)

	Run			
	13	14	15	16
Temperature, K	623	708	723	773
Pressure, atm.	1	1	1	1
Weight of cat. ^a , g	1.0	1.0	1.0	1.0
Toluene, WHSV ^b	9.27	9.27	9.27	9.27
Conversion, %	1.3	3.4	4.4	7.0
Product wt. %				
CH ₄	-	-	-	Traces
Benzene	0.55	1.94	2.3	3.8
Toluene	98.7	96.6	95.6	93.0
Ethylbenzene	-	-	-	Traces
p-xylene	0.360	0.596	0.68	0.956
m-xylene	0.364	0.733	1.01	1.585
o-xylene	0.025	0.13	0.404	0.658
Xylene Isomers, %				
Para	48.10	40.82	32.52	29.88
Meta	48.55	50.22	48.22	49.56
Ortho	3.35	8.96	19.26	20.56

a - 3 mm pellet

b - Weight hourly space velocity: weight of feed per unit weight of catalyst per hour.

APPENDIX-1 (Continued)

	Run			
	17	18	19	20
Temperature, K	773	773	773	773
Pressure, atm.	1	1	1	1
Weight of Cat. ^a ,g	1.0	1.0	1.0	1.0
Toluene, WHSV ^b	3.3	5.2	7.78	9.27
Conversion, %	12.3	10.1	8.3	7.3
Product wt. %				
CH ₄	Traces	Traces	Traces	Traces
Benzene	6.35	5.92	4.14	3.62
Toluene	87.70	89.90	91.70	92.62
Ethylbenzene	-	-	-	-
p-xylene	1.65	1.25	1.22	0.96
m-xylene	3.04	2.30	1.87	1.59
o-xylene	1.26	0.63	1.07	1.21
Xylene Isomers %				
Para	27.73	29.90	29.32	25.87
Meta	51.09	55.02	44.95	41.50
Ortho	21.17	15.07	25.72	32.61

a - Crushed

b - Weight hourly space velocity: weight of feed per unit weight of catalyst per hour.

APPENDIX-1 (Continued)

	Run			
	21	22	23	24
Temperature, K	773	773	773	773
Pressure, atm.	1	1	1	1
Weight of Cat. ^a , g	0.6	0.6	0.6	0.6
Toluene, WHSV ^b	3.3	5.2	7.78	9.277
Conversion, %	12.2	10.5	8.0	7.1
Product wt. %				
CH ₄	Traces	Traces	Traces	Traces
Benzene	6.25	5.75	4.13	4.82
Toluene	87.8	89.5	92.0	92.9
Ethylbenzene	-	-	-	Traces
p-xylene	1.68	1.22	1.153	0.654
m-xylene	3.10	2.19	1.89	1.08
o-xylene	1.38	0.99	0.820	0.459
Xylene Isomers, %				
Para	27.50	27.70	29.80	29.76
Meta	50.46	49.80	49.00	49.40
Ortho	22.04	22.5	21.2	20.9

a - 3 mm pellet

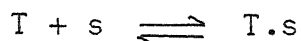
b - Weight hourly space velocity: weight of feed per unit weight of catalyst per hour.

APPENDIX- 2

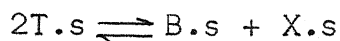
Development of rate expression for Hetrogeneous model:

The following mechanism for the toluene disproportionation reaction has been assumed.

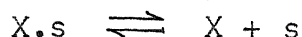
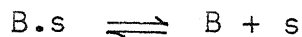
1. Adsorption of toluene on the catalyst surface



2. Surface reaction of the adsorbed molecules to give the adsorbed products



3. Desorption of these adsorbed product molecules to give Benzene and xylene molecules i.e.



Model for adsorption of toluene as the rate controlling step.

A hypothetical P_T^* has been assumed to prevail on the catalyst surface, which is in adsorption-desorption equilibrium. The fractional coverage of the different species can be given by

$$\Theta_T = \frac{K_T P_T^*}{1 + K_T P_T^* + K_B P_B + K_X P_X}$$

$$\theta_B = \frac{K_B P_B}{1 + K_T P_T^* + K_B P_B + K_X P_X}$$

$$\theta_X = \frac{K_X P_X}{1 + K_T P_T^* + K_B P_B + K_X P_X}$$

where θ_T , θ_B , θ_X are the fractional surface coverages of toluene, benzene and xylene respectively. Since the reaction is at equilibrium, the equilibrium reaction constant can be expressed as

$$K_r = \frac{\theta_B \theta_X}{\theta_T^2} = \frac{K_B K_X}{K_T^2} \cdot \frac{P_B P_X}{P_T^{*2}}$$

$$\text{Therefore, } P_T^{*2} = \frac{P_B P_X}{K}$$

Accordingly, the net rate of reaction is

$$\begin{aligned} -r_T &= k_{ad,T} P_T (1-\theta) - k_{de,T} \theta_T \\ &= \frac{k_{ad,T} (P_T - \sqrt{P_B P_X / K})}{(1 + K_T \sqrt{P_B P_X / K} + K_B P_B + K_X P_X)} \end{aligned}$$

Surface reaction rate controlling:

The net rate of reaction is

$$\begin{aligned} -r_T &= K_1 \theta_T^2 - K_2 \theta_B \theta_X \\ &= \frac{K_1 K_T^2 P_T^2 - K_2 K_B K_X P_B P_X}{1 + K_T P_T^* + K_B P_B + K_X P_X} \end{aligned}$$

APPENDIX-3

Rate and partial pressure data for kinetic study

W/F	Conversion ($\frac{X}{\%}$)	$(-r_T \times 10^3)$ gmol/gcat.h.	Partial pressures(atm)		
			P_T	P_B	P_X
T = 623 K					
10	1.6	0.20839	0.2125	0.0019	0.0019
15	2.2	0.17649	0.2889	0.00325	0.00325
20	2.8	0.15734	0.3754	0.01	0.01
27	3.3	0.15195	0.4142	0.014	0.014
T = 708 K					
10	3.5	0.43499	0.2084	0.004	0.004
15	4.7	0.3340	0.2815	0.0069	0.0069
20	5.6	0.25203	0.3646	0.010	0.010
27	6.4	0.16916	0.400	0.014	0.014
T = 723 K					
10	4.5	0.5240	0.2062	0.005	0.005
15	5.9	0.37519	0.2780	0.009	0.009
20	6.9	0.2647	0.3596	0.0133	0.0133
27	7.8	0.1747	0.3949	0.0167	0.0167
T = 773 K					
10	7.2	0.7953	0.2004	0.0078	0.0078
15	9.3	0.5614	0.2679	0.0137	0.0137
20	10.9	0.42952	0.3468	0.0197	0.0197
27	12.4	0.41635	0.3752	0.0266	0.0266

PARAMETERS: X(I)

IN THIS PROGRAMME $X(1) = K_1$; $X(2) = K_T$; $X(3) = K_B$ or K_X

NO OF EXPERIMENTAL POINTS (23) M
NO OF PARAMETERS (2) N
DEPENDENT VARIABLES(1): Y(I)
*****888
INDEPENDENT VARIABLES (2) T(I,J)
STANDARD DEVIATION OF THE PARAMETERS : SD1

DIMENSION FJAC(4,4),FVEC(4),G(100),S(4),V(4,4),W(200)
DIMENSION IW(100),Y(4),PX(4),PA(4),PT(4),PB(4)
DIMENSION PH(4),PI(4),P2(4),PW(4),A(3,3),RA(4)
EXTERNAL LSQFUN,LSQMON
COMMON/DAT/Y,PT,PX,PB
COMMON/VAL/X(4)

M=04
N=4
OPEN(UNIT=6,DEVICE='DSK',FILE='GUPTA.DAT')
READ(31,*) (X(J),J=1,N)
DO 120 I=1,M
READ(31,*) PT(I),PB(I),PX(I),Y(I)
WRITE(21,*) PT(I),PB(I),PX(I),Y(I)
CONTINUE

LI=10
LN=600
LJ=50
LV=8
IPRINT=1
MAXCAL=400*N
ETA=.5
XTOL=10.*SQRT(X02AAF(XTOL))
STEPX=10000.0
WRITE(21,75)
WRITE(21,86) (X(J),J=1,N)
IFAIL=1
CALL EQ4FCE(M,N,LSQFUN,LSQMON,IPRINT,MAXCAL,ETA,XTOL,STEPX,
IX,FSUNSQ,FVEC,FJAC,LJ,S,V,LV,NITER,NF,IW,LIW,W,LW,IFAIL)
WRITE(21,101) IFAIL

```

WRITE (21,102) FSUMSQ
WRITE (21,103) (X(J),J=1,N)
CALL LSQGRD(M,N,FVEC,FJAC,LJ,G)
DO 121 I=1,N
DO 121 J=1,N
A(I,J)=0.0
DO 122 K=1,M
A(I,J)=A(I,J)+FJAC(K,I)*FJAC(K,J)
CONTINUE
DO 600 I=1,N
WRITE (21,103) (A(I,J),J=1,N)
CALL STADEV(X,A,N,M,FSUMSQ)
WRITE (21,105)
WRITE (21,191)
RSS=0.0
SSQ=0.0
DO 40 I=1,M
SS=X(1)*(PT(I)-.07598*PB(I)*PX(I)/PT(I))/
1(1,+X(2)*.07598*PB(I)*PX(I)/PT(I)+
1X(3)*PB(I)+X(4)*PX(I))
FVEC(I)=SS-Y(I)
SSQ=SSQ+(FVEC(I)/Y(I))
RSS=RSS+FVEC(I)**2
WRITE (21,125) SS,Y(I),FVEC(I)
CONTINUE
SS1=SSQ/M
WRITE (21,102) RSS
WRITE (21,110) SSQ
FORMAT(10X,'INITIAL GUESSES FOR REGERSSION'//)
FORMAT(10X,4(2X,E15.8))
FORMAT(//10X,'ERROR EXIT TYPE',I3//)
FORMAT(//10X,'ON EXIT SUM OF SQUARES',E15.8//)
FORMAT(//8X,'AT THE POINT',4E15.8//)
FORMAT(//10X,'THE RESIDUALS ARE'//)
FORMAT(//10X,'ABSOLUTE AVERAGE ERROR=',E15.8//)
FORMAT(5X,60(1H-)/10X,'MODEL VALUE',14X,'EXPT VALUE',
13X,'DIFFERENCE'/5X,60(1H-))
FORMAT(2X,4(8X,E15.8))
END

```

```

*****
SUBROUTINE LSQFUN(IFLAG,M,N,XC,FVECC,IW,LIW,W,LW)

```


page 60

```

DIMENSION FVECC(4),W(200),XC(3),IW(200),PX(4),Y(4),PA(4)
DIMENSION PH(4),PB(4),PT(4),PW(4),RES(4)
COMMON/DAT/Y,PT,PX,PB
COMMON/VAL/X(4)
INTEGER IFLAG,M,N,IW,LIW,LW
DO 20 I=1,M
  ANU=XC(1)*PT(I)*PW(I)
  DEI=((1.+XC(2)*PT(I))*(1.+XC(2)*PW(I)))
  RES(I)=XC(1)*(PT(I)-.2756*SQRT(PB(I)*PX(I)))/
  1((1.0+XC(2)*.2756*SQRT(PB(I)*PX(I))+XC(3)*PB(I))
FVECC(I)=RES(I)-Y(I)
CONTINUE
RETURN
END

```

```

-----
SUBROUTINE LSQMON(M,N,XC,FVECC,FJACC,LJC,S,IGRADE,NITER,NF,IW
1,LIW,W,LW)
DIMENSION FJACC(4,3),FVECC(4),S(2),W(200),XC(2),IW(200),
1G(100)
COMMON/VAL/X(4)
COMMON/DAT/Y,PT,PX,PB
FSUMSQ=F01DEF(FVECC,FVECC,M)
CALL LSQGRD(M,N,FVECC,FJACC,LJC,G)
GTG=F01DEF(G,G,N)
WRITE(21,107) NITER,NF,FSUMSQ,IGRADE
DO 20 J=1,N
  WRITE(21,108)
  FORMAT(/8X,'X',20X,'G',11X,'SINGULAR VALUE'/)
  WRITE(21,109) XC(J)
  FORMAT(/2X,'XC=',2X,E15.8)
CONTINUE
FORMAT(/2X,'ITNS',4X,'FEVALS',10X,'SUMSQ',13X,'GRADE',
12X,14,6X,15,6X,E15.8,2X,I3)
RETURN
END

```

```

+++++
SUBROUTINE LSQGRD(M,N,FVECC,FJACC,LJC,G)
DIMENSION FJACC(4,3),FVECC(4),G(300)
DO 40 J=1,N
  SUM=0.0
  DO 20 I=1,M
    SUM=SUM+FJACC(I,J)*FVECC(I)
  CONTINUE

```

```

      S(J)=SUM+SUM
      CONTINUE
      RETURN
      END
C-----
C----- THE FOLLOWING SUBROUTINE FINDS OUT STANDARD DEVIATION
C-----
      SUBROUTINE STADEV(X,FF,N,M,RSSQ)
      DIMENSION X(4),FF(3,3),FFT(3,3),FY(4),B(10)
      INDIC=-1
      DO 10 I=1,N
      DO 10 J=1,N
10      FFT(I,J)=FF(I,J)
      CALL MATINV(FFT,N,N,B,0,DETERM)
      SIGMA1=RSSQ/(FLOAT(M-N))
      DO 15 I=1,N
      DO 15 J=1,N
      IF(I.EQ.J) GO TO 20
      GO TO 15
20      FFT(I,J)=SIGMA1*FFT(I,J)
      SD2=FFT(I,J)
      SD1=SQRT(ABS(FFT(I,J)))/100.
456      WRITE(21,456)
      FORMAT(10X,'THE FINAL VALUE OF THE PARAMETER'/)
302      WRITE(21,302) J,X(J),SD1,RSSQ
15      FORMAT(10X,'X(',I1,')=',E15.8,3X,'SD1=',E15.8,3X,'RSSQ=',E15.
      CONTINUE
      RETURN
      END
C-----
C----- SUBROUTINE FOR INVERSION OF MATRIX
C-----
      SUBROUTINE MATINV(A,N,IA,B,M,DETERM)
      SUBROUTINE MATINV(A,N,IA,B,M,DETERM)
C*****
C----- SUBROUTINE TO OBTAIN THE INVERSE OF THE MATRIX
C-----
      A(N,N)=INVERSE OF A(N,N)
      DIMENSION A(IA,IA),B(IA,IA),IPIVOT(300),INDEX(300,2)
      EQUIVALENCE (IROW,JROW),(ICOL,JCOL),(AMAX,T,SWAP)
      INITIALISATION
10      DETERM=1.0
15      DO 20 J=1,N
20      IPIVOT(J)=0
      SEARCH FOR PIVOT ELEMENT

```

```

30 DO 550 I=1,N
40 AMAX=0.0
50 DO 105 J=1,N
60 IF(IPIVOT(J)-1) 60,105,60
70 DO 100 K=1,N
80 IF(IPIVOT(K)-1) 80,100,740
90 IF(AMAX-ABS(A(J,K))) 85,100,100
100 IROW=J
110 ICOLUM=K
120 AMAX=ABS(A(J,K))
130 CONTINUE
140 CONTINUE
150 IPIVOT(ICOLUM)=IPIVOT(ICOLUM)+1
160 INTERCHANGE ROWS TO PUT PIVOT ELEMENT ON DIAGONAL
170 IF(IROW-ICOLUM) 140,260,140
180 DETERM=-DETERM
190 DO 200 L=1,N
200 SWAP=A(IROW,L)
210 A(IROW,L)=A(ICOLUM,L)
220 A(ICOLUM,L)=SWAP
230 IF(M) 260,260,210
240 DO 250 L=1,M
250 SWAP=B(IROW,L)
260 B(IROW,L)=B(ICOLUM,L)
270 B(ICOLUM,L)=SWAP
280 INDEX(I,1)=IROW
290 INDEX(I,2)=ICOLUM
300 DIVIDE PIVOT ROW BY PIVOT ELEMENT
310 PIVOT=A(ICOLUM,ICOLUM)
320 DETERM=DETERM*PIVOT
330 A(ICOLUM,ICOLUM)=1.0
340 DO 350 L=1,N
350 A(ICOLUM,L)=A(ICOLUM,L)/PIVOT
360 CONTINUE
370 TF(S) 380,380,360
380 DO 370 L=1,M
390 B(ICOLUM,L)=B(ICOLUM,L)/PIVOT
400 REDUCE NON-PIVOT ROWS
410 DO 550 L1=1,N
420 IF(L1-ICOLUM) 400,550,400
430 T=A(L1,ICOLUM)
440 A(L1,ICOLUM)=0.0
450 DO 450 L=1,N
460 A(L1,L)=A(L1,L)-A(ICOLUM,L)*T

```

```

155 IF(M) 550,550,460
460 DO 500 L=1,M
500 B(L,1)=B(L,L)-B(ICOLUM,L)*T
550 CONTINUE
C INTERCHANGE COLUMNS
600 DO 710 I=1,N
610 L=M+1-I
620 IF(INDEX(L,1)-INDEX(L,2)) 630,710,630
630 JROW=INDEX(L,1)
640 JCOLUM=INDEX(L,2)
650 DO 705 K=1,N
660 SWAP=A(K,JROW)
670 A(K,JROW)=A(K,JCOLUM)
700 A(K,JCOLUM)=SWAP
705 CONTINUE
710 CONTINUE
DO 11 K=1,N
11 IF(IPIVOT(K).NE.1) GO TO 12
CONTINUE
RETURN
12 TYPE 991
991 FORMAT(/30X,'MATRIX IS SINGULAR '/')
740 RETURN
END

```